Phys Chem Minerals (2017) 44:365–375
DOI 10.1007/s00269-016-0864-z

ORIGINAL PAPER

The Mössbauer spectra of prasiolite and amethyst crystals from Poland

Maria Czaja[1] · Mariola Kądziołka-Gaweł[2] · Adam Konefał[2] · Rafał Sitko[3] · Ewa Teper[1] · Zbigniew Mazurak[4] · Michał Sachanbiński[5]

Received: 13 May 2016 / Accepted: 20 November 2016 / Published online: 8 December 2016

Abstract Mössbauer spectroscopy of green (prasiolite) and violet (amethyst) quartz crystals from the Sudety Mountains (Poland) has shown that neither Fe^{2+} nor Fe^{4+} ions are present in them. Only Fe^{3+} ions have been identified and only in interstitial positions in channels parallel or perpendicular to the c-axis. The valence of Fe^{3+} ions did not change as a result of irradiation or annealing. Instead, we believe that the Fe^{3+} ions move within channels or between them.

Keywords Mössbauer spectroscopy · Prasiolite · Amethyst · Fe^{3+} ion

Introduction

Prasiolite is a transparent to translucent quartz variety whose color varies from pale gray green to deep grass green. The first natural prasiolite was found in the early nineteenth century in the vicinity of Suszyna–Mrówieniec (Lower Silesia, Poland) and Płóczki Górne in Lower Silesia, Poland. Other known localities for prasiolite crystals are Montezuma (Southern Bahia, Brazil), Farm Rooisand (Gamsberg, Namibia) and Thunder Bay (Canada). Prasiolite is often accompanied by amethyst in metamorphic, igneous and volcanic glass. Most commercially available samples are artificially produced by heating amethyst from certain locations. These can show zones of amethyst color.

Many studies about the causes of color in varieties of quartz, their changes, and the possibility of the mineral's synthesis have been published. The best known and most often cited are Lehmann and Bambauer (1973), Lehmann (1975), Nassau (1981), Cohen and Sumner (1985), Adekeye and Cohen (1986), Rossman (1994) and Henn and Schultz-Güttler (2012). They have all proven that Fe ions are the main cause of the violet and green color of quartz crystals. The majority of these studies have used mainly spectroscopic methods such as visible (VIS) absorption, infrared and Raman spectroscopy, and electron paramagnetic resonance (EPR). Results based on VIS spectroscopy have appeared in Nunes et al. (2013), on IR spectroscopy in Lamerais (2012) and (Nunes et al. 2013), on EPR spectroscopy in Matarresse et al. (1969), Weil (1984, 1994), Stegger and Lehmann (1989), Halliburton et al. (1989), Han and Choh (1989), Cortezão et al. (2003), SivaRamaiah et al. (2011) and (Nunes et al. 2013).

After Lehmann and Bambauer (1973), Nassau and Prescott (1977) and Rossman (1994), it is widely thought that in colorless quartz, ferric ion (Fe^{3+}) occurs substituting for Si^{4+} at S1 sites in the notation of Lehmann and Bambauer (1973) and at interstitial sites (I_4 sites, ibid.) in the quartz structure. The purple color of amethyst is explained by the formula:

$$Fe^{3+}(S_1) + Fe^{3+}(I_4) \leftrightarrow Fe^{4+}(S) + Fe^{2+}(I_4) \quad (1)$$

✉ Maria Czaja
maria.czaja@us.edu.pl

[1] Faculty of Earth Science, Silesian University, Będzińska 60, 41-200 Sosnowiec, Silesia, Poland

[2] Institute of Physics, Silesian University, Uniwersytecka 4, 40-007 Katowice, Poland

[3] Institute of Chemistry, Silesian University, Szkolna 9, 40-003 Katowice, Poland

[4] Centre of Polymer and Carbon Materials, Polish Academy of Sciences, Skłodowskiej 34, 41-819 Zabrze, Poland

[5] Higher School of Handicraft and Management, St Maciej Square 21, 50-244 Wrocław, Poland

After gamma irradiation, an electron is impelled or released from a substituted Fe^{3+} and trapped by an interstitial Fe^{3+}. By losing the electron, the substituted Fe^{3+} ion is oxidized to Fe^{4+} and the interstitial Fe^{3+} ion is reduced to Fe^{2+}. This electron transition is reversible by heat treatment. Cox (1977) explained polarized absorption spectra of amethyst as connected with d^4 ions—specifically, Fe^{4+}. Cohen (1985) described irradiation-related Fe^{4+} ion located at interstitial rather than substituted sites. Charge transfer among Fe^{4+} and Fe^{2+} ions caused the pleochroic violet color and the intensive absorption band at 545 nm. This electron transition is reversible by heat treatment at 350–450 °C. Moreover, for Fe^{4+} ions, the UV absorption band is at 357 nm. Heat-treated amethyst changes to citrine and at higher temperature (500 °C) to brown quartz caused by Fe_2O_3 particles with an approximate size of 100 nm (Henn and Schultz-Güttler 2012). Certain amethysts can turn to green varieties by heat treatment at 400–500 °C when the interstitial Fe^{3+} (I_4) changes to Fe^{2+} (I_6), showing a wide band at 720 nm. This color is stable up to 600 °C. Color change in different quartz crystals caused by irradiation and heating has been demonstrated mainly with optical, FTIR and Raman spectra (Lameiras et al. 2009; Guttler et al. 2009; Hatipoğlu et al. 2011; Alkmim et al. 2013; Nunes et al. 2013). Nassau and Prescott (1977) found the green and violet colors reflects structurally independent causes and the crystals to be different from "greened amethyst" as described in Lehmann and Bambauer (1973). They observed that green-yellow color of quartz appeared after ^{60}Co gamma irradiation with a dose of 15 megarad (150 kGy). On heating to 350 °C, the violet color was lost, whereas the green color was preserved. The green color was lost on heating to 500 °C and could not be restored by subsequent gamma irradiation. Platonov et al. (1992) showed that the green color of prasiolite is connected with the Fe^{2+}–Fe^{3+} (IVCT) transition which occurred at 725 nm. Herbert and Rossman (2008), in the study of prasiolite crystals from Thunder Bay (Canada), confirmed that the presence of Fe and irradiation of the quartz is necessary to emergence the green color. He also showed that, like amethyst, Thunder Bay prasiolite turned yellow, brown or colorless on heating to >300 °C. Lameiras (2012) showed that colorless quartz crystals could change to prasiolite or amethyst after irradiation with a 400 kGy dose. The irradiation of the colorless sheets was performed in a Cobalt®-60 Nordion GB-127 panoramic dry gamma irradiator up to a dose of 600 kGy. The temperature in the irradiation room was about 300 K (27 °C). The dose rate was not controlled, but it varied from 0.5 to 20 $kGyh^{-1}$.

The valence of the Fe ion, and its position in quartz crystal structure, has been analyzed by EPR spectroscopy in the articles listed earlier. The EPR center is characterized by a gyromagnetic ratio (g factor), which, for a free electron, is the electron g_e factor defined by $\vec{\mu} = g_e \cdot \frac{2 \cdot \pi \mu_B}{h} \cdot \vec{S}$, where $\vec{\mu}$ is the spin magnetic moment, μ_B—Bohr magneton, h—Planck's constant, $\vec{S}$—spin angular momentum. The g factor of a free electron is $g_e = 2.0023$. The g factor of the iron-group ions in crystals, for which the crystalline field is stronger than the spin–orbital interaction, is $g = g_e - \frac{8 \cdot \lambda}{\Delta}$, where λ is the spin–orbital coupling constant and Δ is the strength of the crystalline field. The crystalline field creates through the spin–orbital interaction an additional field of axial or rhombic symmetry. For this reason, the spectrum is described by two $g\perp$ and $g\|$ values for trigonal and tetragonal local symmetry or by three principal g_x, g_y, g_z values for lower crystal symmetry. For ions in low-symmetrical (rhombic and lower) crystalline fields with large initial splitting, measurements at frequencies that are below the splitting value enable one to gather the following information on the ion: site symmetry, the degree of distortion, orientation of the crystalline field axes, the presence of nonequivalent positions. These data are made available by studying the relation of the E/D (rhombicity/axiality) factor. For Fe^{3+} (d^5 ion) spectra measured using the X-band spectrometer, only the $-\frac{3}{2} \rightarrow +\frac{3}{2}$ transition is obtained and the g factor varies from 0–6, taking an isotropic value 4.3 with E/D = 1/3 (Marfunin, 1979). For non-Kramers ions (Fe^{2+} or Fe^{4+}), obtaining the EPR spectra is feasible only with a small splitting in the zero field. In fields of orthorhombic or lower symmetry fields, only singlet levels remain, and moreover, the distance between them exceeds the microwave quantum $h\nu$ in use and no EPR signal for the X-band spectrometer is observed.

The EPR measurements for amethyst crystals proved that ferric (Fe^{3+}) ions are present in substituted orthorhombic sites with a g factor of about 4.28 (SivaRamaiah et al. 2011) and in interstitial sites, in channels, with a g factor close to 2.0023. Research conducted by Weil (1984, 1994) has proven that Fe^{3+} ions in amethyst are present in tetrahedral sites and are accompanied by different positive ion compensators (Li, Na, H), with g factors close to 2.00 and different E/D factors. The distribution of Fe^{3+} ion in three Si^{4+} equivalent sites could be unequal, as described by Cortezão et al. (2003). Cox (1976) used measurements of amethyst done with K and Q—band spectrometers to prove the presence of not only the Fe^{3+} ion but also of Fe^{4+} in the crystals studied. Moreover, Stegger and Lehmann (1989) admit the possibility that some EPR signals could be caused rather by Fe^{2+} or Fe^{4+} ions. EPR measurement of prasiolite shows, above all, lines originating from E' centers, as well as a broad line, characteristic for Fe^{3+}, at $g = 2$ (Sachanbiński et al. 1994; Sachanbiński and Jezierski 2015). The authors also suggested the possibility of Fe^{2+}–O^- interaction and the formation of Fe^{3+}–O^{2-} pairs.

Mössbauer spectroscopy is the most suitable method for researching the valence and coordination of Fe ions and is used most often for Fe-bearing minerals. Examples of the many good publications on the application of Mössbauer spectroscopy to the study of minerals are those of Greenwood and Gibb (1971), Zhe et al. (2001), Darby Dyar et al. (2006), Berry (2005), Grodzicki and Lebernegg (2011), Golubeva et al. (2009) and Fridrichova et al. (2015). Mössbauer spectra characterize the iron ions through the following parameters: isomer shift (IS), quadrupole splitting (QS) and half line width (Γ). The isomer shift parameter (IS or δ) where $IS = \alpha \cdot (\rho_0^{\text{Sample}} - \rho_0^{\text{Reference}})$ is a measure of the density of *s*-electrons at the nucleus compared with their density at the source nucleus. It is proportional to the electron density ρ_0 at the nucleus. Constant α is proportional to the change of the nucleus radii during the transition. For the Fe^{57} nucleus, the positive isomer shift corresponds to a decreased electron density on the nucleus. The *s*-electron density, however, becomes subject to an effect produced by the 3*d*-electrons of iron—an effect that manifests itself in the shielding the *s*-electrons on the nucleus. Thus, any increase in the number of the d-electrons leads to a reduction of the *s*-electron density at the nucleus and, consequently, to a greater isomeric shift. So Fe^{3+} ions have a lower isomer shift than Fe^{2+} as ρ_0 of Fe^{3+} is greater due to a weaker screening effect by the *d*-electrons. Quadrupole splitting (QS or Δ) is a product of a nuclear quadrupole moment *Q* times electric field gradient V_{zz} and electron charge *e* $QS–eQV_{zz}$. The electric field gradient depends on local distortion of the Fe-site and interaction of ligand electrons with intrinsic *p*- and *d* -electrons of the atom. For Fe^{3+} and high-spin state, five *3d*-electrons form a half-occupied shell with a spherical symmetry and, thus, the intrinsic Fe^{3+} electrons fail to contribute to the quadrupole splitting. In this case, the quadrupole splitting is dominated by the lattice contribution. For high-spin Fe^{2+} (d^6 configuration), the crystal field and lattice distortion in the nucleus site should be noted. The quadrupole splitting parameter is frequently large for slightly distorted sites (Evans et al. 2005a, b). A comparison of the value of the quadrupole splitting with the degree of coordination polyhedron distortion generally shows no unequivocal interdependence (Ingalls 1964; Rancourt et al. 1994).

The isomer shift (IS) for different coordination numbers is $^{VIII}Fe^{2+} > 1.20$ mms^{-1}, $^{VI}Fe^{2+} > 1.05–1.20$ mms^{-1}, $^{IV}Fe^{2+} > 0.80–1.05$ mms^{-1}, $Fe^{2.5} > 0.55–0.80$ mms^{-1}, $^{VI}Fe^{3+} > 0.35–0.55$ mms^{-1}, $^{IV}Fe^{3+} > 0.15–0.35$ mms^{-1}, and, for Fe^{4+}, it varies from −0.2 mms^{-1} to 0.02 mms^{-1} (Burns and Solberg 1990). Quadrupole splitting (QS) for Fe^{4+}, Fe^{3+} and Fe^{2+} ions in an ideal cubic environment equals zero. The asymmetry of the lattice electric field causes the splitting of the excited $I = 3/2$ level, and, generally, QS for Fe^{2+} is considerably greater than QS for Fe^{3+}. Furthermore, the more distorted the coordination polyhedron surrounding the Fe^{3+} ions, the larger the QS becomes.

This is a question about the detection limit of Fe by Mössbauer spectroscopy. Ali-Zade et al. (1987) proposed a theoretical formula calculating the lowest concentration of Fe atoms whose signal can be reliably recorded in samples containing atoms of a single element. For Al, Cu and Zr matrices, they obtained values 10^{-3}, 10^{-2} and $3 \cdot 10^{-2}$ atomic percent, i.e., 10, 100 and 300 ppm, respectively. So it is possible to measure the resonance signal for samples of SiO_2 (with the light elements Si and O) containing several Fe ppm. This assumption was proven for synthetic amethyst by Dedushenko et al. (2004) and for fulgurites by Sheffer (2007). They measured repeatable Mössbauer spectroscopy results for SiO_2, containing relatively little Fe, i.e., 160 ppm (Dedushenko et al. 2004) and 400 ppm (Sheffer 2007). However, Sheffer (2007) detailed the conditions of measurements more completely than Dedushenko (2004) did. Deduschenko et al. (2004) prepared an artificial amethyst (with about 160 ppm Fe) which was gamma irradiated with a dose of 1 Gys^{-1}. They measured a single line with an isomer shift of 0.00 mms^{-1}. This result confirmed the thesis that the violet color in quartz structure reflected the presence of Fe^{4+}.

In this paper, we present here the results of Mössbauer spectroscopy measurements for a prasiolite from Sokołowiec, Poland, and four violet quartz crystals from Sokołowiec, and from other sites in Poland. All the quartz samples were gamma irradiated (dose 10 kGy), heat treated (500 °C/2 h), and the irradiated ones were also heated. In this manner, the five quartz samples were prepared for Mössbauer spectroscopy. The data were augmented by XRF analyses. As the iron content in the quartz crystals was very low, the Mössbauer spectroscopy measurements were conducted over many (<9) days to order to obtain the most accurate results possible.

The aim was to confirm the presence of Fe^{2+} and Fe^{4+} in prasiolite and amethyst, respectively. However, the results of did not confirm their presence.

Materials and methods

At Sokołowiec, prasiolite with an intense green color forms crystals that completely or partially fill amygdales in porphyritic volcanic rocks. The prasiolite is genetically related to well-known agate occurrences. A dark amethyst (Sample A2a) and another with a bright amethyst color (Sample A2b) were also collected at this locality. Amethyst (Sample A3) Tertiary agates at Regulice near Kraków and amethyst (Sample A1) from a quartz vein in slate in the Kletno massif (Sudety Mountains) were also analyzed.

Table 1 Chemical composition of studied and related quartz samples

	Prasiolite Sokołowiec	A2a Amethyst dark Sokołowiec	A2b Amethyst bright Sokołowiec	A1 Amethyst Kletno	A3 Amethyst Regulice	Other amethyst crystals	Prasiolite Brazil[d]	Prasiolite Suszyna[e]
Fe_2O_3 (%)	0.2390	0.0065	0.0018	0.0120	0.0130			
Fe ppm	836	23	6	42	45	From 1 to 2.5 $\times 10^{4a}$ 100[b] >50[c] 30–140[d]	3–17	1000
Cr (ppm)	4.5	–	–	–	–	0.01[a]	<4	–
Mn (ppm)	5.0	3.1	–	45.8	–	<0.1[a]	2.5	100.0
Cu ppm)	3.2	2.9	3.3	3.0	2.6	3–18[a]	–	10.0
Zn (ppm)	3.4	3.1	–	–	–	6–66[a]	–	10.0
Sn (ppm)	–	–	–	–	–	–	–	–
Ga (ppm)	1.7	–	–	19.8	–	1–20[a]	–	–
Ge (ppm)	2.9	–	–	1.6	–	–	–	5
As (ppm)	–	–	–	–	–	<1–9[a]	–	–
Sr (ppm)	–	3.7	–	–	4.5	1–6[a]	–	–
Ba (ppm)	21.7	–	–	–	–	1–56[a]	–	–
Be (ppm)		–	–	–	–	–	–	10.0
B (ppm)		–	–	–	–	–	–	55.0

Data from [a] Hatipoglu et al. (2011), [b] Cohen and Sumner (1985), [c] Cortezão et al. (2003), [d] Lameiras et al. (2009), [e] Sachanbinski et al. (1994)

Chemical analyses

Chemical analyses were performed using an energy-dispersive X-ray fluorescence (EDXRF) spectrometer—Epsilon 3 (Panalytical, Almelo, Netherlands) with a Rh target X-ray tube operated at a maximum voltage of 30 keV and a maximum power of 9 W. The spectrometer is equipped with a thermoelectrically cooled silicon drift detector (SDD), with a 8-μm Be window and a resolution of 135 eV at 5.9 keV. Quantitative analysis was performed using Omnian software based on a fundamental parameter method and under the following measurement conditions: 12 kV, 300 s counting time, helium atmosphere, 50-μm Al primary beam filter for Ba; 20 kV, 120 s counting time, air atmosphere, 200-μm Al primary beam filter for Cr, Mn and Fe; 30 kV, 120 s counting time, air atmosphere, 100-μm Ag primary beam filter for Cu, Zn, Ga, Ge, As, Sr and Y. The current of the X-ray tube was fixed to not exceed a dead-time loss of ca 50%. The results are presented in Table 1.

Irradiation procedure

The samples were irradiated using 6 megavolt X-rays from a medical linear accelerator. All samples received a dose of 10 kGy. A special system (8 cm × 8 cm × 8 cm plastic box) was built for this irradiation. The surface of the box was placed 60 cm from the X-ray source. The samples were located 1.75 cm below the box surface facing the radiation source. In the plastic, X-rays are characterized by the specific dose distribution with the maximum dose at depths of ca 1.5 to 2 cm. In this manner, the irradiation of the sample was controlled very accurately; dose uncertainty was <2%. The maximum energy value was 6 MeV, and the average energy value of the photons beam was 0.5 MeV. Moreover, the irradiation method used ensured homogeneity of dose distribution throughout the sample (Konefał et al. 2015).

Heat treatment

The prasiolite sample was heated at 500 °C/1 h and 600 °C/8 h. After the first step of annealing, the green crystals did not change color, but the colorless ones became brown. After heating at the higher temperature, the green crystals became bright yellow, and those that had become brown earlier became colorless again.

The amethyst crystals were heated at 500 °C for 2 h in an air atmosphere in static conditions. After heating, amethyst crystals with higher Fe content (A1 and A3) changed their color to bright citron-like yellow, but the amethysts from Sokołowiec (A2a and A2b) became colorless. After irradiation, the color of the studied amethysts did not change, although the hue of the color of sample A3 did so to a small degree.

Mössbauer measurements

The ^{57}Fe Mössbauer spectra were recorded at room temperature using a constant acceleration spectrometer with a

Table 2 Mössbauer doublets assignments for prasiolite crystal (IS—isomer shift, QS—quadruple splitting, G—line width, A—relative intensity)

Sample	Component	IS (mms^{-1})	QS (mms^{-1})	G (mms^{-1})	A (%)
Initial	D1 Fe^{3+} (trig)	0.148	0.568	0.28	29.0
	D2 Fe^{3+} (tetra)	0.188	0.342	0.30	61.0
	D3 Fe^{3+} (octa)	0.331	0.176	0.24	10.0
Irradiated	D1 Fe^{3+} (trig)	0.138	0.480	0.24	31.0
	D2 Fe^{3+} (tetra)	0.198	0.348	0.26	52.0
	D3 Fe^{3+} (octa)	0.364	0.210	0.22	17.0
Annealed	D1 Fe^{3+} (trig)	0.140	0.470	0.24	32.0
	D2 Fe^{3+} (tetra)	0.199	0.356	0.26	52.0
	D3 Fe^{3+} (octa)	0.372	0.194	0.22	16.0
Irradiated and annealed	D1 Fe^{3+} (trig)	0.132	0.490	0.26	39.0
	D2 Fe^{3+} (tetra)	0.205	0.356	0.24	43.0
	D3 Fe^{3+} (octa)	0.366	0.232	0.32	18.0

^{57}Co:Rh source (activity ~ 15 mCi), a multichannel analyzer with 1024 channels and a linear arrangement of the ^{57}Co source, absorber and detector. A gas proportional counter was used as the gamma-ray detector. A 2-mm plastic filter was placed in the beam to absorb the 6 keV X-rays before they enter the detector. The 2 keV escape peak and 14.4 keV γ ray pulses were selected with a multichannel analyzer. A metallic iron powder (α-Fe) absorber was used for velocity and isomer shift calibration of the Mössbauer spectrometer. The numerical analysis of the Mössbauer spectra was performed with the use of the WMOSS program. The obtained spectra were fitted as a superposition of several doublets. The decomposition into doublets was performed by a Lorentzian function. The time of Mössbauer spectrum collection was typically from four to nine days, and baseline counts ranged from ~25 to 50 million after the Compton correction, as required to obtain reasonable counting statistics. No influence by the detector window on the spectrum was not observed during the period of the measurements. For the prasiolite and amethyst crystals, the error for the IS parameter was from 1 to 15%, the mode 4%, the average 6%. The error for the QS parameter was from 1 to 11%, the mode 4%, average 5%. The highest values of errors, e.g., 15 and 11%, pertain to the hyperfine parameters of one sub-spectra of the bright amethyst from Sokołowiec (A2a). The results for prasiolite are shown in Fig. 2a–d and in Table 2 and those for the amethyst crystals in Fig. 3a–d and in Table 3. The resonance signal of the bright amethyst sample (A2b) is very weak but does not contain any false or random counts and neither does the signal from detector window measured under the same condition, as demonstrated in Fig. 4.

Results and discussion

The Fe content in the prasiolite crystal from Sokołowiec is significantly greater than in the other crystals (Table 1). In the amethyst crystals, the contents were average or lower. Levels of residual elements are similar to those reported in Hatipoğlu et al. (2011).

Demonstrating the occurrence of the Fe^{4+} as well as Fe^{2+} ions would be a huge import to an understanding of the cause of color of amethyst and prasiolite. In that context, a review of all possible sites for iron ions in the quartz structure is pertinent.

1. The S sites lie on a twofold axis, and their charge compensator is an unidentified alkali ion or OH replacing oxygen. The size of the Si–O tetrahedra indicates that substitutional sites are appropriate mainly for Fe^{3+} ions and Fe^{4+}. The presence of Fe^{2+} ions in S sites is hard to accept, up to now, has not been confirmed as because Fe–O distances are 1.911 and 1.8645 Å (mincryst database), i.e., they are greater than for Si–O in quartz (1.598 and 1.616 Å).
2. Some interstitial positions are located in channels in the quartz structure. Quartz has relatively open channels. The large central channel is parallel to the threefold c-axis and formed by a six-membered ring of SiO_4 tetrahedra. The average size of this channel in $a_{1,2,3}$-direction is about 3.28 Å. It is widely accepted, after Lehmann and Bambauer (1973), that there exist two different interstitial sites for ions coordinated by four or six oxygen ions and denoted as I_4 or I_6, respectively (Fig. 1a). The I_4 site has coordination number 4; the effective D_2 symmetry and oxygen–I_4 distances are: O(3)-I_4 = 2.57 Å, O(5)-I_4 = 2.34 Å. For the I_6 site with coordination number 6 and effective C_s symmetry and the oxygen–I_6 distances are O(1)-I_6 = 3.02 Å, O(3)-I_6 = 2.42 Å and O(5)-I_6 = 2.34 Å. Six small three-membered rings with the average size about 2.68 Å and C_{3v} symmetry (Fig. 1b) are placed around this central channel. The site in that channel is marked as I_3 on Fig. 1b. This site is smaller than ones previ-

Table 3 Mössbauer doublets assignment for studied amethyst crystals

Sample	Component	IS (mms^{-1})	QS (mms^{-1})	G (mms^{-1})	A (%)
Amethyst (A1); Kletno					
Initial	D1 Fe^{3+} (tetra)	0.183	0.415	0.33	77.0
	D2 Fe^{3+} (octa)	0.311	0.175	0.24	23.0
Irradiated	D1 Fe^{3+} (tetra)	0.174	0.375	0.40	79.0
	D2 Fe^{3+} (octa)	0.359	0.233	0.31	21.0
Annealed	D1 Fe^{3+} (tetra)	0.146	0.396	0.38	73.0
	D2 Fe^{3+} (octa)	0.365	0.294	0.28	27.0
Amethyst dark (A2a); Sokołowiec					
Initial	D1 Fe^{3+} (tetra)	0.176	0.404	0.32	82.0
	D2 Fe^{3+} (octa)	0.361	0.120	0.22	18.0
Irradiated	D1 Fe^{3+} (tetra)	0.193	0.406	0.28	84.0
	D2 Fe^{3+} (octa)	0.335	0.007	0.22	16.0
Annealed	D1 Fe^{3+} (tetra)	0.185	0.410	0.28	79.0
	D2 Fe^{3+} (octa)	0.310	0.131	0.22	21.0
Irradiated and annealed	D1 Fe^{3+} (tetra)	0.169	0.376	0.28	82.0
	D2 Fe^{3+} (octa)	0.404	0.062	0.22	18.0
Amethyst bright (A2b); Sokołowiec					
Initial	D1 Fe^{3+} (tetra)	0.137	0.401	0.34	57.0
	D2 Fe^{3+} (octa)	0.317	0.319	0.28	43.0
Irradiated	D1 Fe^{3+} (tetra)	0.148	0.389	0.33	58.0
	D2 Fe^{3+} (octa)	0.311	0.287	0.30	42.0
Annealed	D1 Fe^{3+} (tetra)	0.101	0.417	0.30	44.0
	D2 Fe^{3+} (octa)	0.307	0.334	0.31	56.0
Amethyst (A3); Regulice					
Initial	D1 Fe^{3+} (tetra)	0.147	0.382	0.33	68.0
	D2 Fe^{3+} (octa)	0.324	0.308	0.27	32.0
Irradiated	D1 Fe^{3+} (tetra)	0.074	0.405	0.35	43.0
	D2 Fe^{3+} (octa)	0.312	0.346	0.33	57.0
Annealed	D1 Fe^{3+} (tetra)	0.175	0.405	0.30	72.0
	D2 Fe^{3+} (octa)	0.311	0.222	0.28	28.0

ously discussed and has a bigger distortion. If it is assumed that *x*/*a*, *y*/*a* and *z*/*c* of the I_3 site are 0.50, 0.33 and <0.66 (e.g., 0.583), respectively, and the distances are O(1)-I_3 = 2.55 Å, O(3)-I_3 = 2.17 Å and O(5)-I_3 = 1.99 Å, and Fe^{3+} ion could be placed in this small channel. The average distance between the I_4 site in the channel and the I_3 site in the small channel is 1.89 Å.

3. The other channel is parallel to the a_i-axis, halfway between two equivalent silicon sites in the c-direction (Fig. 1c). The site in the middle of this channel is coordinated like the I_4 site in the c-channel, that is, by oxygen numbered as O(3)- and O(5). Therefore, in these cases, the effective symmetry and the Fe–O distances are the same. These large c- and a-channels intersect in site I_4.
4. Other channels intersect with the c- and a-axis channels and make an angle of about 57° with the c-axis. It has been known for a long time that small positive ions H^+, Li^+ and Na^+ can be present in these and can diffuse readily throughout them.

It is worth considering the possibility of a displacement of iron ions over small distance within the different sites of individual channels or among channels. The preferred site for such a displacement is site the I_4 site in the central c-channel. Displacement parallel to the c-axis from this site to I_6 would seem to be easy, and the distance between I_4 and I_6 is only 0.900 Å. Displacement in a perpendicular direction along the a-channel does not change the Fe–O bond length or the symmetry of coordination polyhedra. Only displacement from I_4 to I_3 causes a distinct decrease in Fe–O bond length and diminishes the symmetry of coordination. Such a displacement, though for a distance of 1.89 Å that is twice greatest than I_4—I_6, is not hindered either by the silicon site or by O(1) ions. Such displacements might well be achieved by the heating or irradiation of crystals.

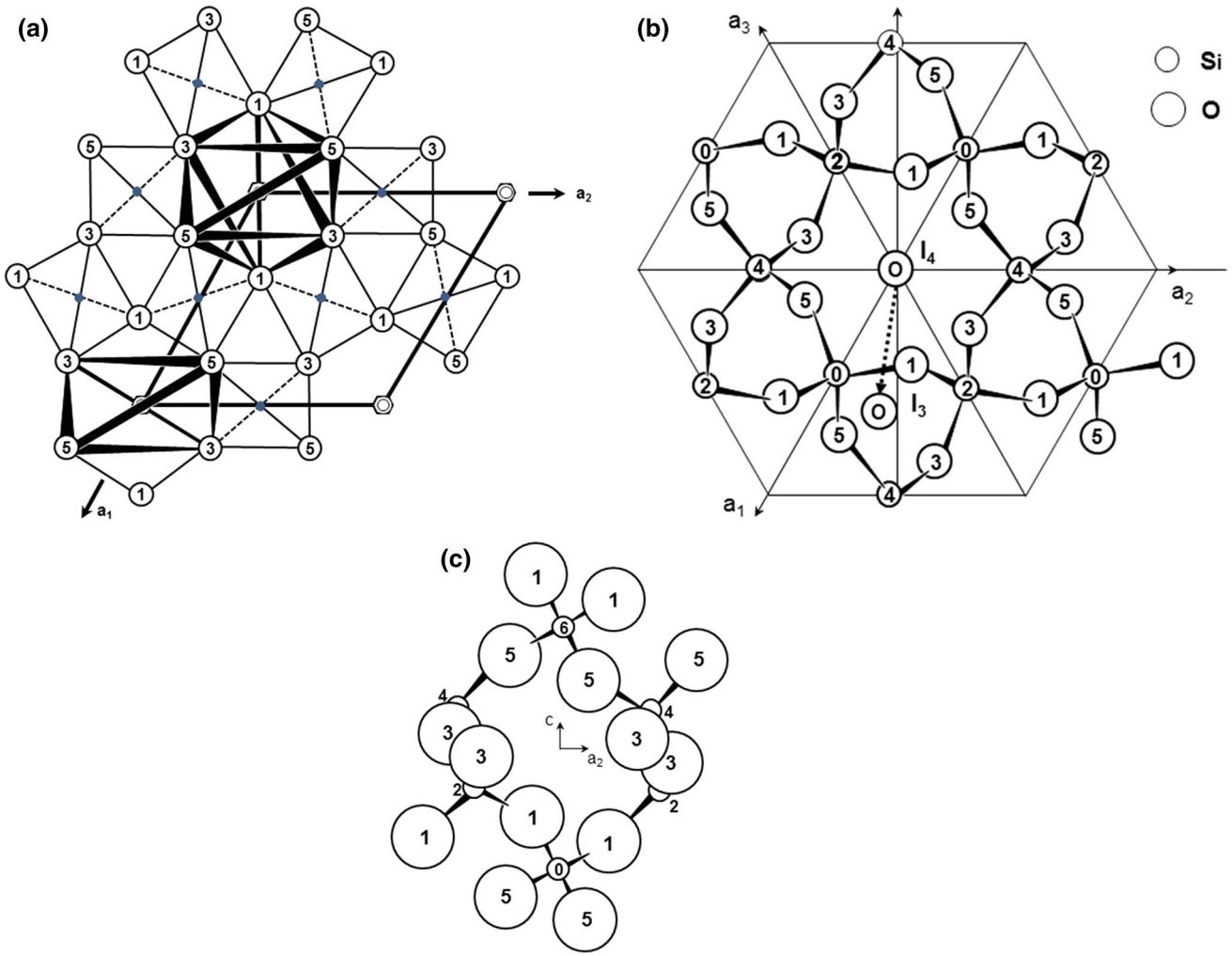

Fig. 1 Simplified sketches of the quartz structure. The number in the circle is approximately equal to coordinate *z*/*c*. **a** After Fig. 1 in Lehmann and Bambauer (1973). **b** Projection onto plane perpendicular to the *c*-axis; view onto the *c*-channel after Fig. 1 in Weil et al. (1984). **c** Projection onto plane perpendicular to the a_1-axis; view onto the *a*-channel after Fig. 9 in Matarresse et al. (1969)

It is thought that the possible result of irradiation and heating is the change of valence state from Fe^{3+} to Fe^{4+} and/or Fe^{2+}, as well as changes in bonding lengths and the symmetry of coordination polyhedron. For this reason, distinct changes in quadrupole shift (QS) and isomer shift (IS) would be expected. However, we propose that the moving of Fe ions from interstitial sites be considered. It has been shown for amorphous silica (Agnello 2000), and calculated for the quartz (Wang et al. 2015), that the average threshold displacement energy is 28.9 and 70.5 eV for oxygen and silicon, respectively, and that the displacement is <10 Å. Also, an EPR study (Hirai and Ikeya 1998) has shown that the heating at 600 °C led to the displacement of atoms, and formed an oxygen vacancy around Si–O tetrahedra. If such effects can emerge for strongly bonded Si–O atoms, it seems more than likely that, with the treatments described in this paper, they can emerge for weakly bonded Fe ions from interstitial sites.

Consider the Mössbauer spectra for prasiolite from Sokołowiec. These are presented in Fig. 2a–d and in Table 2, for primary (Fig. 2a) and irradiated (Fig. 2b) samples, as well as for those heated at 500 °C (Fig. 2c) and for those which were both irradiated and heated (Fig. 2d). In this prasiolite, only the Fe^{3+} ion has been identified. It is evident from the data in Table 2 that Fe^{2+} ions are present neither in the primary nor in the irradiated or heated crystal. Instead of its ion, three doublets have been singled out. One, marked as D3, corresponds to the Fe^{3+} ions in the octahedral site; it is probably the I_6 site. The two remaining doublets (D2 and D1) should be assigned to Fe^{3+} ions in tetrahedral sites due to their smaller isomer shift values and larger quadrupole shift values. The doublet D1 has a smaller IS than D2, which is characteristic for a smaller Fe-ligand distance. For this reason, the D1 doublet could initially be considered as originating from Fe^{3+} ions substituting silicon in the

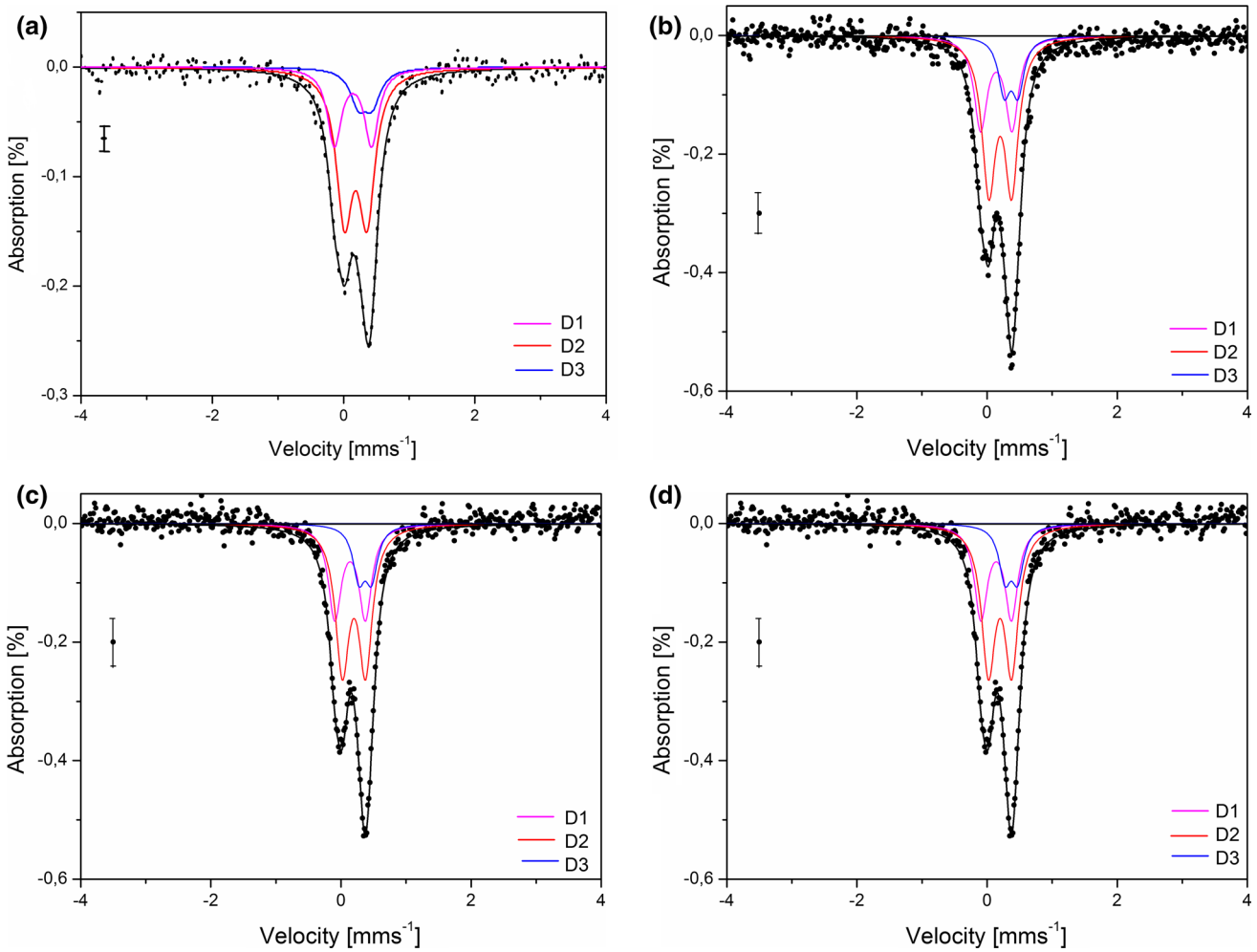

Fig. 2 Mössbauer spectra of prasiolite; **a** primary crystal, **b** irradiated crystal, **c** annealed crystal, **d** irradiated and then annealed crystal. The number of doublets and the color of the components correspond to those in Table 2

quartz structure, and D2 from Fe^{3+} in interstitial I_4 sites. This assumption, however, is difficult to reconcile with the fact that the quadrupole splitting of D1 is distinctly larger than that of D2. Distortions of the SiO_4 polyhedron calculated according to the formulas in Robinson et al. (1971) are equal, i.e., 6.17×10^{-5} for Si–O in the quartz structure and 6.27×10^{-4} for the I_4 site. Thus, the need is to find other sites for which both conditions, namely the smallest Fe–O distances and the largest distortions of coordination, would be met. In our opinion, the I_3 site meets these conditions. Therefore, we conclude that all Fe ions are Fe^{3+} and are situated in the interstitial positions; they are in sites I_4 and I_6 of the big channel; in the small channel (site I_3), they appear on the spectra as doublets D2, D3 and D1. The effects of irradiation and heating confirm this conclusion. The isomer shift (IS) and the quadrupole splitting (QS) decrease for doublet D1 and increase for doublets D2 and D3, and the half-width decreases for all components. This means that the bond lengths and symmetry of the coordination polyhedra have changed in a similar manner for ions of doublet D2 and D3, but differently for those of doublet D1. The central big channel increases in dimension at the expense of the smaller channel. As a result of irradiation and heating, a change in the filling of individual sites has occurred. The amount of iron in tetrahedral sites I_4 decreases in stark contrast to that in sites I_6 and I_3. The distance between these sites is 0.90 Å along the c-axis from I_4 to I_6 or 1.89 Å perpendicular to the c-axis from I_4 to I_3. The shift from site I_4 to I_6 appears to be easier; thus, the number of Fe^{3+} ions moving from I_4 to I_6 is greater than from I_4 to I_3.

The contents of iron in the amethyst samples are twenty to forty times smaller than in the prasiolite. For all of the amethyst crystals, only two doublets (D1 and D2) were observed; their parameters are presented in Table 3 and Fig. 3a–d. These doublets are identified as corresponding to Fe^{3+} ions' tetrahedral and octahedral coordination. The presence of Fe^{4+} ions has not been confirmed in any of the samples. The amount of Fe^{3+} ions in the tetrahedral site is

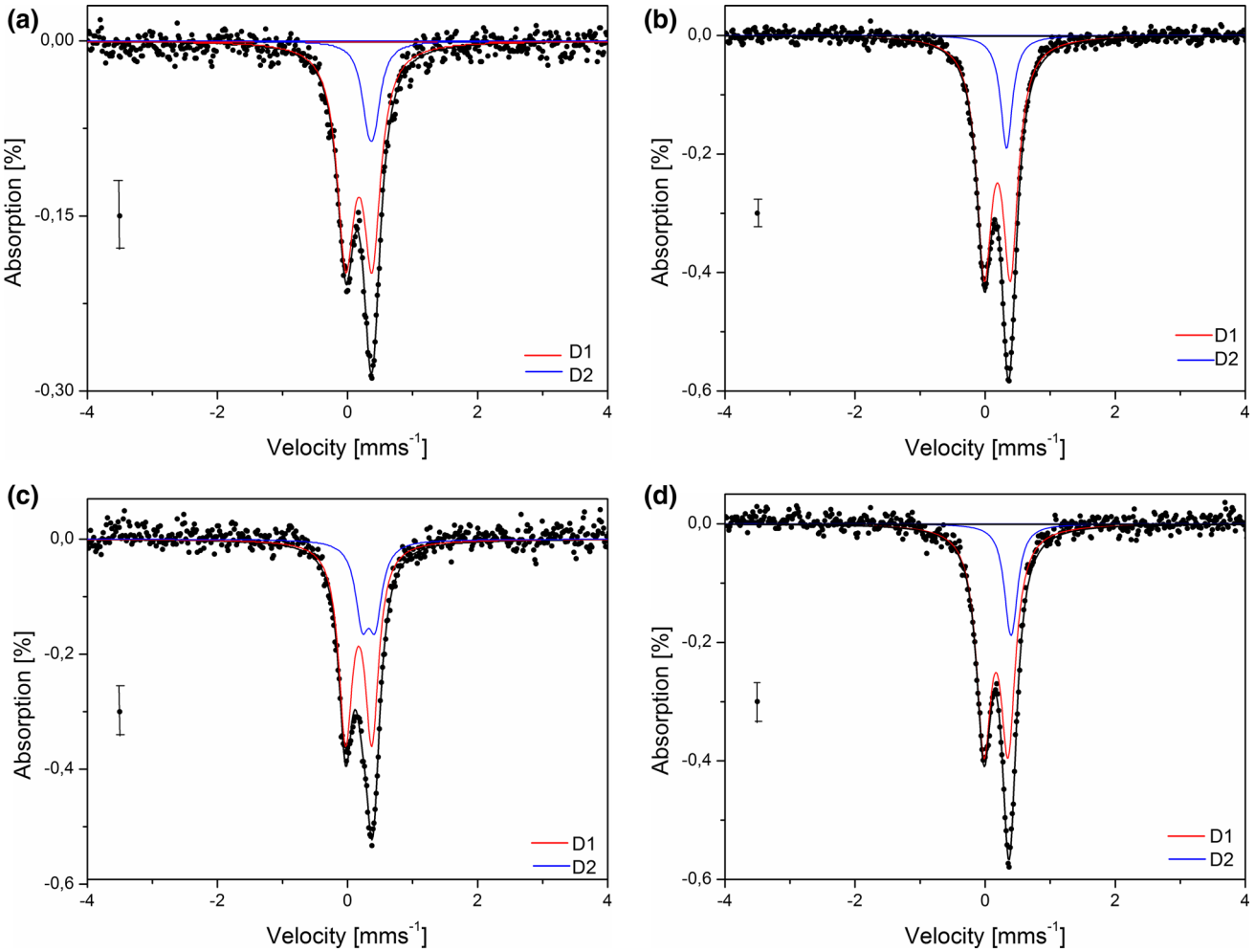

Fig. 3 Mössbauer spectra of the amethyst crystals from Sokołowiec (*dark violet color*); **a** primary crystal, **b** irradiated crystal, **c** annealed crystal, **d** irradiated and then annealed crystal. The number of doublets and the color of the components correspond to those in Table 3

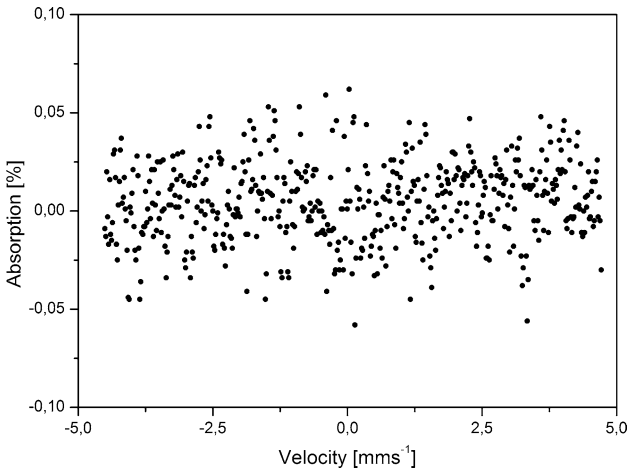

Fig. 4 Mössbauer spectrum of the detector windows measured over 10 days

distinctly greater than in the octahedral site. The fact that the half-width of the D1 doublet is greater than that of the doublet D2 means that the lattice neighborhood of Fe^{3+}_{tetra} ions in this position is not identical. The IS and QS parameters of doublet D2 are similar to those of doublet D3 of prasiolite; therefore, we conclude that Fe^{3+}_{octa} ions are present in the c-channel in the I_6 site. For the identification of the site (or sites) of Fe^{3+}_{tetra}, the following hypotheses merit consideration.

(a) Fe^{3+}_{tetra} ions in samples A2b and A3 substitute for Si^{4+} ions in the quartz crystal structure as the IS parameter is lower than it is for the other amethysts. However, we see a contradiction in this assumption is evident when the volatility, on heating and irradiation, of the quantities of those ions in a tetrahedral and octahedral coordination is noted. The possibility of the presence of Fe^{3+} ions substituting for Si^{4+} must therefore be rejected.

(b) All Fe^{3+}_{tetra} ions are present in interstitial sites in different channels, in sites such as I_4 in the prasiolite of samples A1 and A2a, and I_3 in that of prasiolite for A2b and A3. However, the similar QS parameters for all samples do not accord with this hypothesis. Furthermore, the displacement of Fe^{3+} ion from I_3 after heating or irradiation is very difficult and has not been observed.

(c) Fe^{3+}_{tetra} ions are present in interstitial sites in different channels, in sites such as I_4 of prasiolite for A1 and A2a amethyst, but for amethyst in A2b and A3, they are present in the a-channel. It has been noted above that the dimension of the a-channel is less than that of the c-channel, but the axial distortion appears to be similar. This assumption meets the requirement of the similar values of the QS parameter. In addition, the ions in the two channels are mobile and weakly bonded with the Si–O crystal structure.

For samples A1 and A2a, no regular changes of the IS or QS parameters have been observed, nor has any quantitative participation of Fe^{3+} in a tetrahedral and octahedral coordination resulting from the irradiation or heating. After irradiation, quantitative Fe^{3+} participation in the octahedral I_3 site increased somewhat, and after heating, it decreased. Slightly more pronounced changes of the IS and QS parameters and relative intensity (A in Tables 2, 3) have been observed for the A2b and A3 samples (Fe^{3+}_{tetra} in the a-channel). The A value for tetrahedral Fe^{3+} is greater than for octahedral Fe^{3+}, particularly in samples A1 and A2a. Moreover, the changes of A after heating and irradiating are significant. For sample A2b, they occurred after heating, and for sample A3, after irradiation. In addition, these changes are accompanied by a doublet with IS parameters very close to zero (0.101 ± 0.007 and 0.074 ± 0.017, respectively). Initially, one could hypothetically assume a presence of Fe^{4+} ions in some unknown quantity, but why this effect was produced under different conditions is not evident. However, the fact that the value of the QS parameter is close to zero, but not exactly equal to zero, strongly suggests that this assumption is wrong. Therefore, after heating or irradiation, Fe^{3+} ions move into positions with shortened bond lengths, probably within the same channel. This may explain why IS decreases and QS increases.

Conclusions

1. In the search of Fe^{2+} and Fe^{4+} ions in the studied prasiolite and amethyst crystals, only Fe^{3+} ions were actually found.
2. The Fe^{3+} ions are present only as interstitial ions in different sites in channels parallel or perpendicular to the c-axis.
3. Because these ions are rather weakly bonded with the Si–O crystal structure, they can move on heating or irradiating.
4. For samples with small contents of Fe, measurements performed over several days enabled satisfactory results to be obtained.
5. The quartz crystals studied by us did not, in any way, exhibit the same behavior previously attributed to similar crystals by others; as neither Fe^{2+} ion occurs in the prasiolite, nor Fe^{4+} ion in the amethyst, the reason for their color remains an open question.

Acknowledgements This research project was supported by the Polish National Science Centre (Grant DEC-2011/03/B/ST10/06320) and by statutory funding from the Faculty of Earth Sciences, University of Silesia. Dr. Padhraig S. Kennan (University College Dublin, Ireland) helped with language correction and authors thank him very much.

References

Adekeye JID, Cohen AJ (1986) Correlation of Fe^{4+} optical anisotropy, Brazil twinning and channels in the basal plane of amethyst quartz. Appl Geochem 1:153–160

Agnello S (2000) Gamma ray induced processes of point defect conversion in silica. Dissertation, Università di Palermo. www.unipa.it/lamp/AgnelloPhDThesis

Ali-Zade II, Babikova YF, Vakar OMYu, Petrikin V (1987) Evaluation of the detection limit in electron-recording Mössbauer spectroscopy. Sov Phys J 30:738–740. doi:10.1007/BF00897470

Alkmim DG, Lameiras FS, Almeida FOT (2013) Identification of color development potential of quartz by Raman spectroscopy. INAC 2013, Recife, PE Brazil, *ISBN:* 978-85-99141-05-2

Berry FJ (2005) Mössbauer Spectroscopy. Cambridge University Press, Cambridge, p 270

Burns RG, Solberg CT (1990) Crystal structure trends in Mossbauer spectra of ^{57}Fe-bearing oxide, silicate, and aluminosilicate minerals. In structure of active sites in minerals. ACS Symp Ser 415:262–283

Cohen AJ (1985) Amethyst color in quartz, the result of radiation protection involving iron. Am Mineral 70:1180–1185

Cohen AJ, Sumner GG (1985) Relationships among impurity contents, color centers and lattice constants in quartz. Am Mineral 43:58–68

Cortezão SU, Pontuschka WM, Da Rocha MSF, Blak AR (2003) Depolarization currents (TSDC) and paramagnetic resonance (EPR) of iron in amethyst. J Phys Chem Solids 64:1151–1155

Cox RT (1976) ESR of an S = 2 Centre in amethyst quartz and its possible identification as d^4 ion Fe^{4+}. J Phys C 9:3355–3361

Cox RT (1977) Optical absorption of the d^4 Fe^{4+} in pleochroic amethyst quartz. J Phys C 10:4631–4643

Darby Dyar M, Agresti DG, Schaefer MW, Grant CA, Sklute EC (2006) Mössbauer spectroscopy of earth and planetary materials.

Annu Rev Earth Planet Sci 34:83–125. doi:10.1146/annurev.earth.34.031405.125049

Dedushenko SK, Makhina IB, Mar'in AA, Mukhanov VA, Perfiliev YUD (2004) What oxidation state of iron determines the amethyst colour? Hyperfine Interact 156(157):417–422

Evans RJ, Rancourt DG, Grodzicki M (2005a) Hyperfine electric field gradients and local distortion environments of octahedrally coordinated Fe^{2+}. Am Mineral 90:187–198

Evans RJ, Rancourt DG, Grodzicki M (2005b) Hyperfine electric gradient tensors at Fe^{2+} sites in octahedral layers: toward understanding oriented single-crystal Mössbauer spectroscopy measurements of micas. Am Mineral 90:1540–1555

Fridrichova JP, Rusinova P, Antal P, škoda R, Bizovska V, Miglierini M (2015) Optical and crystal-chemical changes in aquamarines and yellow beryls form Thanh Hoa province, Vietnam induced by heat treatment. Phys Chem Miner 42:281–301. doi:10.1007/s00269-014-0719-4

Golubeva OYU, Semenov VG, Volodin VS and Gusarov VV (2009) Structural Stabilization of Fe4 + Ions in Perovskite-Like Phases-Based on the BiFe–SrFeO*y* System. Glass Phys Chem + 35:13–319. Original Russian Text © O.Yu. Golubeva, V.G. Semenov, V.S. Volodin, V.V. Gusarov, 2009, published in Fizika i Khimiya Stekla. ISSN 1087-6596

Greenwood NN, Gibb TC (1971) Mössbauer Spectroscopy. Springer, p 605; ISBN: 978-94-009-5699-5. doi:10.1007/978-94-00905697-1

Grodzicki M, Lebernegg S (2011) Computation and Interpretation of Mössbauer parameters. In: P. Gutlich, E.Bill (ed) Mossbauer Spectroscopy and Transition Metal Chemistry. Fundamentals and Application. A.X. Trautwein Ch. II.2 pp 1–102 extras.springer.com. doi:10.1007/978-3-540-88428-6

Guttler RAS, Enokihara CT, Rela PR (2009) Characterization of color centers in quartz induced by gamma irradiation. International nuclear Atlantic conference—INAC 2009, Rio de Janeiro, Brazil, ISBN: 978-85-99141-03-8

Halliburton LE, Hantehzadeh MR, Minge J, Mombourquette MJ, Weil JA (1989) – EPR study of Fe^{3+} in α—quartz: a reexamination of the lithium-compensated center. Phys Rev B 40:2076–2081

Han CS, Choh SH (1989) EPR study of iron centers in natural amethyst. J Korean Phys Soc 22:241–252

Hatipoğlu M, Kibar R, Çetin A, Can N, Helvaci C, Derin H (2011) Spectral, electron microscopic and chemical investigations of gamma-induced purple color zonings in amethyst crystals from Dursunbey-Balikesir region of Turkey. Radiat Eff Defects S 166:537–548

Henn U, Schultz-Güttler R (2012) Review of some current coloured quartz varieties. J Gemm 33:29–43

Herbert LB, Rossman GR (2008) Greenish quartz from the Thunder Bay amethyst mine panorama, Thunder Bay, Ontario, Canada. Can Mineral 4:61–74. doi:10.3749/canmin.46.1.000

Hirai M, Ikeya M (1998) Narrowing of ESR spectra of E' center in crushed quartz by thermal annealing. Phys Status Solidi B 209:449–462

http://www.mincryst

http://www.quartzpage.de

Ingalls R (1964) Electric-field gradient tensor in ferrous compounds. Phys Rev A 133:787–795

Konefał A, Bakoniak M, Orlef A, Maniakowski Z, Szewczuk M (2015) Energy spectra in water for the 6 MV X-ray therapeutic beam generated by Clinac-2300 linac. Radiat Meas 72:12–22. doi:10.1016/j.radmeas.2014.11.008

Lameiras FS (2012) The Relation of FTIR signature of natural colorless quartz to color development after irradiation and heating. In: Morozhenko V (ed) Infrared radiation. InTech, ISBN: 978-953-51-0060-7. doi:10.5772/35738

Lameiras FS, Nunes EHM, Vasconcelos WL (2009) Infrared and chemical characterization of natural amethysts and prasiolites colored by irradiation. Mater Res -Ibero-Am-J 12:315–320. doi:10.1590/S1516-14392009000300011

Lehmann G (1975) On the color centers of iron in amethyst and synthetic quartz: a discussion. Am Mineral 60:335–337

Lehmann G, Bambauer HU (1973) Quartzkristalle und ihre Farben. Angew Chem 85:281–289

Marfunin AS (1979) Spectroscopy, luminescence and radiation centers in minerals ch. 3 Electron paramagnetic resonance. Springer, Berlin, pp 76–118 352

Matarresse LM, Wells JS, Peterson RL (1969) EPR spectrum of Fe^{3+} in synthetic brown quartz. J Chem Phys 50:2350–2360

Nassau K (1981) Artificially induced color in amethyst-citrine quartz. G&G Spring 17:37–39

Nassau K, Prescott BE (1977) Smoky, blue, greenish yellow, and other irradiation-related colors in quartz. Mineral Mag 41:301–312

Nunes EHM, Lameiras FS, Houmard M, Vasconcelos WL (2013) Spectroscopic study of natural quartz samples. Radiat Phys Chem 90:79–86

Platonov AN, Sachanbiński M, Ignatov SI (1992) Natural prasiolite from Lower Silesia, Poland. Z Dt Gemmol Ges 41:21–27

Rancourt DG, Pink JY, Berman RG (1994) Mössbauer spectroscopy of minerals. III. Octahedral-site Fe^{2+} quadrupole splitting distribution in the phlogopite-annite series. Phys Chem Minerals 21:258–267

Robinson K, Gibbs G, Ribbe PH (1971) Quadratic elongation: a quantitative measure of distortion in coordination polyhedra. Science 172:567–570

Rossman GR (1994) Colored varieties of the silica minerals. In Haney PJ (ed) Review in mineralogy and geochemistry silica: physical behavior, geochemistry, and materials applications. 29:433–463

Sachanbiński M, Jezierski A (2015) New data on prasiolite. Gemmołogija i kamen w architekturie. http://h.120-bal.ru/geografiya/1814/index.html?page=45

Sachanbiński M, Platonov A, Jezierski A (1994) Nowe dane o prasiolicie. Prace Specjalne PTMin 197–199

Sheffer AA (2007) Chemical Reduction of Silicates by Meteorite Impacts and Lightning Strikes. PhD Thesis Faculty of the Department of Planetary Sciences, University of Arizona,p 245

SivaRamaiah G, Lin J, Pan Y (2011) Electron paramagnetic resonance spectroscopy of Fe^{3+} ions in amethyst: thermodynamic potentials and magnetic susceptibility. Phys Chem Miner 38:159–167

Stegger P, Lehmann G (1989) The Structures of three centers of trivalent iron in α- quartz. Phys Chem Miner 16:401–407

Wang B, Yu Y, Pignatelli I, Sant GN, Bauchy M (2015) Nature of radiation-induced defects in quartz. J Chem Phys 43:1–8. doi:10.1063/1.4926527

Weil JA (1984) A Review of electron spin spectroscopy and its application to the study of paramagnetic defect in crystalline quartz. Phys Chem Miner 10:149–165

Weil JA (1994) EPR of iron centers in silicon dioxide. Appl Magn Reson 6:1–16

Zhe LI, Shinno I, Danian YE, Pingqiu FU, Yueming Z (2001) A Mossbauer effect study of Fe^{3+} bearing γ Fe_2SiO_4. Sc China Ser D 44:34–46